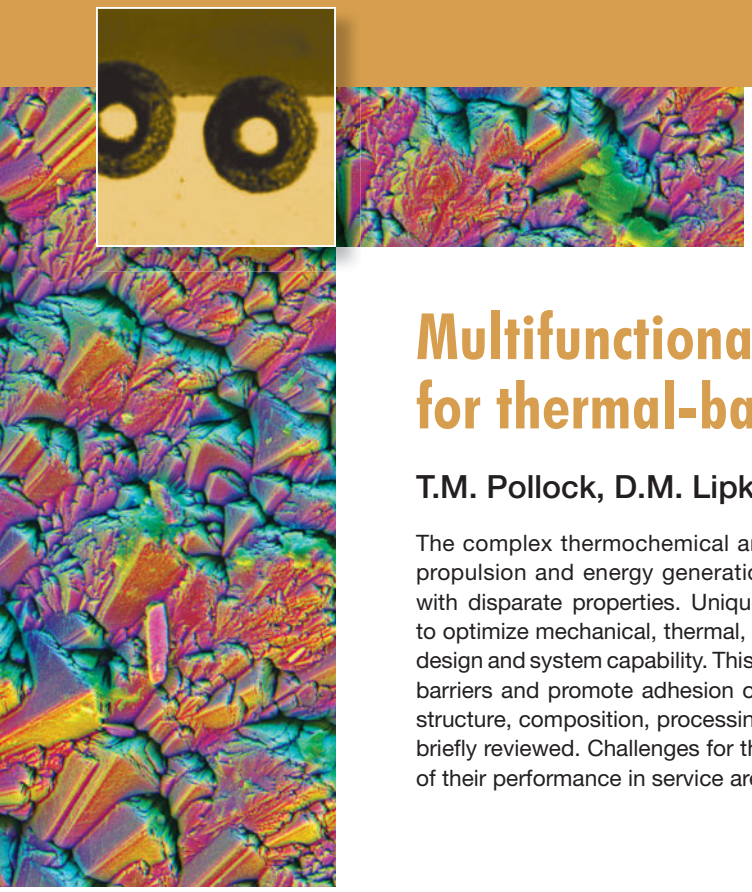


Multifunctional coating interlayers for thermal-barrier systems

T.M. Pollock, D.M. Lipkin, and K.J. Hemker

The complex thermochemical and thermomechanical environments in high temperature propulsion and energy generation systems often demand the use of suites of materials with disparate properties. Unique combinations of materials that simultaneously function to optimize mechanical, thermal, and environmental properties can enable breakthroughs in design and system capability. This article focuses on interlayers that function as environmental barriers and promote adhesion of the ceramic thermal barriers to metallic substrates. The structure, composition, processing, and performance of major classes of bond coatings are briefly reviewed. Challenges for the development of new coating systems and for prediction of their performance in service are addressed.

Introduction

Thermal-barrier systems are an excellent example of multilayered, multifunctional material assemblies that have enabled substantial improvements in the performance and efficiency of gas turbine engines. The combination of a metallic substrate, an intermetallic (or mixed metallic and intermetallic) interlayer, and a low conductivity ceramic topcoat permits the system to operate near, or even above, the melting point of the substrate in a highly oxidizing combustion environment.[1–7]

Intermetallic coatings have long been a central requirement for high temperature operation of propulsion and power generation systems. In early applications in aero- and land-based turbines (before ceramic thermal barriers were developed), environmental coatings typically served a single function. Aluminide-type coatings based on NiAl and NiCoCrAl-family coatings became the standard systems for oxidation protection, while diffusion chromides and overlay CoNiCrAl materials were used to protect against hot corrosion.[1,6] As turbine operating temperatures have increased, fuels have become cleaner, substrate alloys have evolved to refractory-rich nickel-based single crystals, and environmental coatings have become (by necessity) multifunctional. In current turbine components (see Figure 1 in the introductory article for a depiction of a gas turbine), a single coating deposited on a turbine blade may be expected to:[1–9]

- Resist Type II hot corrosion in cooler sections (e.g., in blade shanks).
- Resist Type I hot corrosion in intermediate-temperature regions (e.g., below the blade platform and in cooler sections of airfoils).
- Resist high-temperature oxidation in the hottest sections (e.g., blade tips, platforms, and airfoils).
- Maintain adhesion to the thermal-barrier coating (TBC).
- Provide environmental protection in the event of TBC spallation.
- Minimize interdiffusion and limit transformations at the interface with the nickel-based substrate.

The challenges of developing intermetallic bond coatings that will reliably perform in present and future engineering systems are addressed in this article. A perspective on presently available bond coating systems and their functionality is given first. The suite of processing approaches for interlayer synthesis and challenges in controlling structure and composition are then addressed. Aspects of the bond coating that limit system performance are reviewed. New experimental and characterization tools and computational design approaches are highlighted, along with future prospects for discovery of new materials combinations and for prediction of their performance in complex thermo-chemical-mechanical environments.

T.M. Pollock, Materials Department, University of California, Santa Barbara; Pollock@engineering.ucsb.edu
D.M. Lipkin, GE Global Research, Fairfield, CT; lipkin@ge.com
K.J. Hemker, Department of Mechanical Engineering, Whiting School of Engineering, The Johns Hopkins University; hemker@jhu.edu
DOI: 10.1557/mrs.2012.238

© 2012 Materials Research Society

https://doi.org/10.1557/mrs.2012.238 Published online by Cambridge University Press

Structure, functionality, and classes of bond coatings

The intermetallic bond coat exists as an intermediate layer between the metallic substrate (typically a nickel-based superalloy) and the ceramic top coating (typically yttria-stabilized zirconia). The thickness of the bond-coat layer is typically between 30–100 μm, varying in thickness as a function of processing approach and service time. The bond coating is chemically complex due to the need to optimize a broad set of thermomechanical and thermochemical properties.

Given that bond coatings are deposited on Ni-based substrates and upon high temperature exposure from surface films of either chromia or alumina, the Ni-Al-Cr ternary diagram at 1100°C, **Figure 1**, is relevant. In the ternary compositional space, phases that exist include the B2 β phase with approximately equal levels of Ni and Al, the fcc γ-Ni and γ-Al phases, the $L1_2$ γ′–Ni_3Al phase, and the A2 α-Cr phase. These phases are often present in as-deposited coatings. Bond coatings can be broadly classified by these major phase constituents.[1,2,7] Coatings comprised primarily of the B2 β phase are typically referred to as "nickel aluminide" coatings, and if they additionally contain platinum are classified as "platinum aluminides." A combination of the β and γ′ phases forms the basis of "MCrAlY" coatings, where the "M" often refers to Ni, Co, or a combination of both. Several emerging coating systems contain a γ′ phase with some level of γ–Ni present.

The high temperature processing paths for application of the coatings, discussed in more detail in the next section, inevitably include interdiffusion with the substrate, resulting in an interdiffusion zone that may contain several additional refractory-rich phases. Moreover, the bond-coat structure evolves by interdiffusion during high temperature exposure, potentially resulting in further phase transformations and/or migration of elements that are detrimental to system performance (**Figure 2**). Calculated phase diagrams for higher order multicomponent systems can be useful for avoiding the formation of brittle intermetallic phases in this zone and for designing thermal treatments that follow coating application. Given the operating environments for these coatings, control of both the thermodynamic and kinetic properties is essential.

The bond coating must serve as an environmental barrier for the substrate due to the fact that the outer, low conductivity ceramic is permeable to oxygen. Consequently, the ability to form a dense, protective oxide in the operating environment is one of the primary requirements of the bond coating. Most of the intermetallics presently employed as bond coatings contain a sufficiently high level of aluminum to promote the formation of a dense α-Al_2O_3 layer at the surface of the bond coat adjacent to the TBC, which has a relatively slow growth rate and is resistant to degradation by any corrosive species that reach the surface through the thermal barrier, or subsequent to spallation of the ceramic thermal barrier.[2–9] The thin oxide layer is typically referred to as the thermally grown oxide (TGO). Given the high temperature operating requirements, it is essential that the TGO be thermodynamically compatible with the ceramic thermal barrier. To achieve the protective requirements, the bond coating must serve as a chemical reservoir for TGO formation, as well as a diffusion barrier or diffusion sink for any deleterious refractory elements from the superalloy substrate that may degrade the bond-coat properties or the bond coat—TGO interface adhesion.[10–14] While the TGO provides the coating system with an oxidation benefit, this thin interlayer may also endure large thermal and growth stresses that challenge the durability of the layered TBC system when exposed to severe thermal transients characteristic of turbine airfoils, as discussed in more detail later.

To be effective over the life span of the turbine component for which the bond coating is intended to protect the substrate, it must also be thermochemically and thermomechanically compatible with the substrate so as to prevent—or at least limit—debits to the mechanical properties of the load-bearing components. At present, coatings are still not relied upon to provide load-bearing capability, though this may be on the horizon for the next generation of coatings. In addition to their functional requirements, the coatings must be applied using processes that are cost effective, capable of providing the required thickness and chemical homogeneity, and compatible with other processes or thermal operations required for component fabrication. These requirements drive the development of new coating compositions, architectures, and the processes to fabricate them, discussed in the following section.

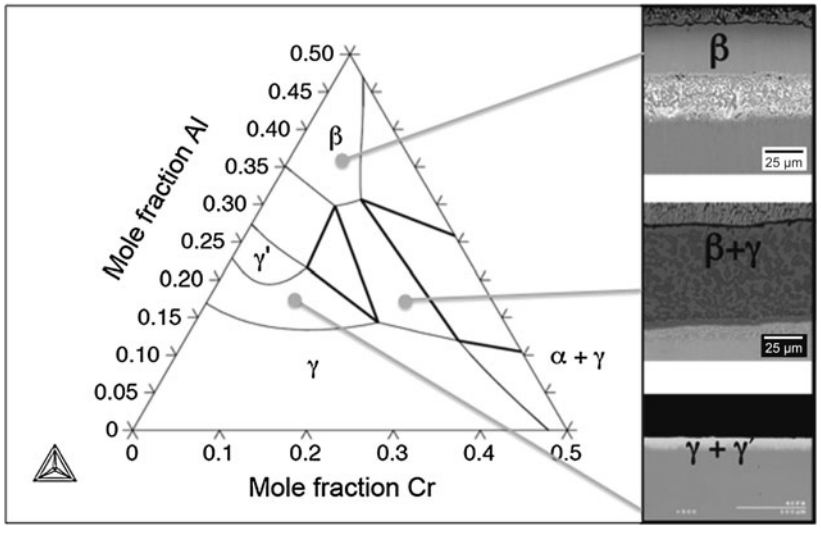


Figure 1. Ternary Ni-Al-Cr phase diagram predicted by the Calphad method, and approximate compositions of three different bond coating classes shown in scanning electron micrographs on the right. Shifts in the amounts of Al, Cr, and Ni in these coatings permit changes in the predominant phase.

https://doi.org/10.1557/mrs.2012.238 Published online by Cambridge University Press

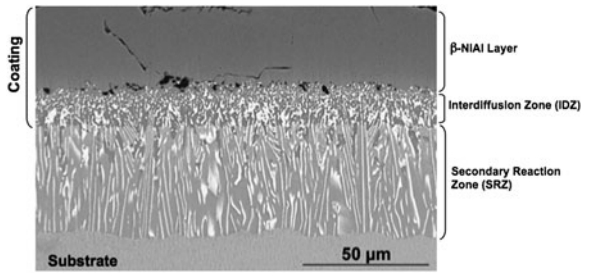


Figure 2. Interdiffusion-induced cellular transformation that results in detrimental intermetallic phases in a secondary reaction zone as a result of deposition of a NiAl coating on a Ni-5.9Al-5.6Ru-7.9Ta-7.4Re-2.9W-2.3Co-6.6Cr (wt%) substrate. This zone continues to grow into the substrate.

Coating application: A multiplicity of processing paths

As coating compositions have evolved to keep up with the functional demands of engineering components, so too have the processes for depositing them. While coating compositions can be optimized solely on their chemical and microstructural characteristics, it is essential to have a coating process capable of uniformly covering the complex geometries of the turbine components and compatible with all subsequent manufacturing processes, such as TBC deposition, heat treatments used to establish braze joints, and any heat treatments used to establish the desired substrate properties. The challenge of delivering ever-increasing coating functionality while maintaining robust and cost-effective manufacturing processes has led to a multiplicity of coating processes, which may be broadly classified into two categories: diffusion coatings and overlays.

Diffusion coatings

Diffusion coatings, particularly aluminide coatings, are the product of interdiffusion between the superalloy component and an aluminum source (donor). The simplest of these processes, and the earliest to be industrially implemented, is pack cementation,[15] schematically illustrated in **Figure 3**a. Components to be aluminized are embedded into a mixture of the aluminum source, an inert matrix (typically alumina sand), and a halide salt activator (e.g., AlF_3 or NH_4F). The aluminum sources can be elemental aluminum or aluminum-containing alloys, such as CrAl, CoAl, or NiAl. Alloy donors are used to increase the donor melting temperature and define the chemical activity of aluminum, allowing the coating microstructures to be tuned for improved performance. The pack is located in a retort and heated to temperatures in the range 650–1200°C in a non-oxidizing atmosphere, such as argon or hydrogen. On heating, the halide activator transports aluminum from the donor to the surface of the target component, where it decomposes, releasing aluminum to diffuse into the alloy and cycling the halide back to the donor to pick up more aluminum. At temperatures above ~1050°C and with packs having low-aluminum activity donors, NiAl coatings form via predominantly outward diffusion of the nickel from the substrate. These coatings are typically single-phase and have Al:Ni ratios less than unity. For pack aluminizing at temperatures below ~1000°C, and especially when the packs have high-activity donors (e.g., metallic aluminum), coatings grow by predominantly inward diffusion of aluminum.

Aluminizing processes employing long-range vapor-phase transport of the aluminum source have also been developed, eliminating the need to place components directly in the pack. These processes are generally categorized as vapor-phase aluminizing (VPA) and chemical vapor deposition (CVD). In both cases, the components to be coated are placed in a high-temperature retort, and the aluminum-bearing vapors are transported to them by an inert gas.[16] This allows both external and internal surfaces to be coated. In VPA, the aluminum source, or donor alloy, is usually a refractory alloy of aluminum; examples include CrAl, CoAl, NiAl, and Ti_2AlC-TiAl (also known as Codep donor).[17,18] A halide salt (e.g., AlF_3, NH_4F, NaF, and mixtures thereof) is used as an activator to destabilize the native oxide and initiate vapor-phase transport transfer of aluminum.

In CVD aluminizing,[6] the aluminum source is injected into the heated retort as a precursor gas in a non-oxidizing carrier gas. The precursor can be delivered directly from a tank source (e.g., as $AlCl_3$) or by passing anhydrous halide, such as HCl or HF, over an aluminum donor at a controlled temperature, pressure, and flow rate, so as to form the corresponding volatile halide salts (e.g., $AlCl_3$ or AlF_3). Because each process has some advantages (and limitations) over the other, both VPA and CVD continue to be employed in industrial applications.

Additional environmental performance benefits can be gained by incorporating other elements into the aluminide coating. Elements including Cr, Si, Hf, Zr, and Y have been incorporated into diffusion aluminide coatings to impart enhanced resistance against corrosion, cyclic oxidation resistance, or improvement in TBC retention.[15,19,20] One of the most widely adopted durability enhancements to the simple aluminide (on external surfaces only) is platinum-modified nickel

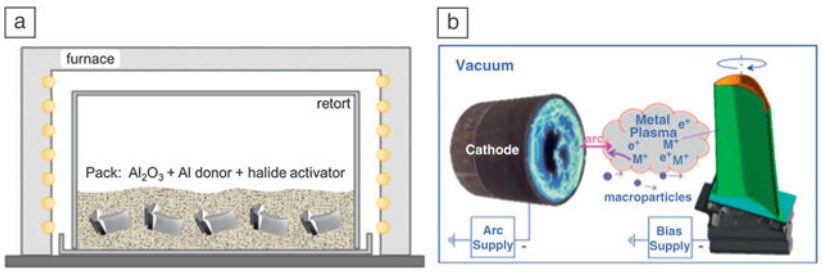


Figure 3. (a) Schematic of a pack cementation system, consisting of a high-temperature retort surrounded by a furnace. The parts are embedded in a pack consisting of an inert filler (typically alumina), donor (e.g., CrAl alloy), and halide activator (e.g., AlF_3). (b) Schematic of an ion plasma deposition process in which molten droplets and ionized vapor are ejected from a metal cathode to coat the part (shown in green).

https://doi.org/10.1557/mrs.2012.238 Published online by Cambridge University Press

aluminide.[21–24] These coatings are typically synthesized in a three-step process, consisting of electroplating 5–10 μm of platinum and an inert-atmosphere interdiffusion heat treatment, followed by a diffusion aluminizing process (pack or vapor phase), as described previously. In an additional variant of the platinum diffusion coatings, direct platinizing of the superalloy, without a subsequent aluminizing step, has also been demonstrated to improve the environmental resistance and TBC bond-coating performance of turbine alloys.[25–28]

While the processes for making simple and alloyed diffusion aluminides are widely used in the manufacture of turbine components, the degree to which their microstructures and thicknesses can be specified is limited by the phase equilibrium and diffusion kinetics inherent to the reactant-superalloy system. Whereas diffusion aluminides are still the standard for all internal coatings, external coatings are therefore also applied using overlay processes, as described later.

Overlay coatings

Overlay coatings provide the flexibility of tailoring the composition of complex, multi-component systems without the compositional and thickness constraints inherent to the diffusion coatings. Because thermal spray deposition processes have been most broadly applied to environmental and bond coatings, these are described first.

Simple MCrAl-family coatings can be deposited by a number of processes, producing varying degrees of coating density and process-induced oxidation.[29] As interest in the incorporation of reactive element additions (e.g., Hf, Y, Zr, and Si) into the MCrAl-based coatings has increased, inert-atmosphere processes have been employed to prevent tying up these elements with oxygen during deposition. Physical vapor deposition in vacuum, namely electron-beam physical vapor deposition (EBPVD), can deposit high-quality MCrAls with reactive element additions.[30] While EBPVD and other physical vapor deposition processes have several appealing features, including their ability to deposit clean, dense coatings containing highly reactive elements, these processes involve costly equipment and maintenance and throughput-limiting sample exchange protocols. As a result, low-pressure plasma spray (LPPS) has emerged as a lower-cost alternative and is broadly used.[31]

LPPS systems carry the burden of high cost associated with the accompanying vacuum chamber. In this regard, the emergence of atmospheric deposition processes, including inert-gas shrouded plasma spray[32,33] and high-velocity oxyfuel (HVOF),[34] has made the high-volume deposition of complex MCrAls with reactive elements routine.[35] The trend toward simultaneously reducing particle temperatures while increasing particle velocities has continued with the emergence of new processes, such as activated combustion high-velocity air fuel (HVAF)[34,36] and cold-gas dynamic spraying (cold spray).[37,38] These processes enable the atmospheric deposition of dense coatings with limited oxidation of the most reactive elements.

An emerging trend in process technologies is the hybridization of what used to be considered distinct deposition mechanisms in order to synergistically benefit from the advantages of multiple processes. Recent examples include very-low pressure plasma spray[39] and ion plasma deposition (Figure 3b).[40–42] These processes combine the benefits of droplet-based deposition (fast, clean, amenable to transferring multi-component chemistries) with those of physical vapor deposition (dense, adherent, chemically homogeneous). Yet another hybrid process that has been employed to improve the failure resistance of bond coatings is the over-aluminizing (by either overlay, pack diffusion, or out-of-pack diffusion processes) of MCrAl-family and NiAl-family coatings.[6] It is anticipated that these as well as new combinations of conventionally distinct processes will continue to be explored.

Coating properties and performance

Bond coatings are key to TBC system durability and require a complex combination of thermal, mechanical, and environmental properties to maintain adherence of the ceramic top layer. For example, bond-coat creep strength, thermal misfit with the superalloy substrate, and TGO growth strains strongly influence three major intrinsic failure modes: rumpling, edge delamination, and sustained peak low cycle fatigue (see Figure 1 in the Levi article in this issue).[43–45] A major challenge lies in the measurement and prediction of the physical and mechanical properties of the interlayers that compose the coating system to increase resistance to these failure modes and maximize system life. As described later, some of the relevant properties of the most common coating systems have been measured. Unfortunately, property measurement is rarely incorporated as a tool for developing new generations of coatings. As described in the section on "New design and characterization tools," there are emerging characterization techniques that may permit more systematic development of coating systems.

With thermal excursions exceeding 1000°C, differences in the coefficients of thermal expansion (CTEs) of the coating relative to the superalloy substrate of only 1 μstrain °C^{-1} generates thermal stresses on the order of hundreds of MPa—stresses that are high enough to promote bond-coat plasticity at elevated temperatures and interfacial delamination upon cool down.[9] The CTEs of bulk materials are readily measured using a dilatometer, but measuring the CTE of thin films extracted from the various layers of a thermal-barrier system requires alternative techniques. Non-contact digital image correlation provides one route to measuring the CTE of thin films as a function of temperature; **Figure 4** compares CTE measurements for a standard diffusion aluminide bond coat with those for a standard commercial single crystal superalloy substrate, René N5. Differences in CTE of approximately 2 μstrain °C^{-1} are present at room temperature, but this difference varies over the temperature range of interest and reverses at high temperature. Comparison of the CTE for commercial MCrAlY bond coats and their substrates do not exhibit a reversal, but differences of 2 to 3 μstrain °C^{-1} are not uncommon and are generally exacerbated at the highest temperatures. To more closely match the expansion characteristics of the superalloy substrate, coatings

https://doi.org/10.1557/mrs.2012.238 Published online by Cambridge University Press

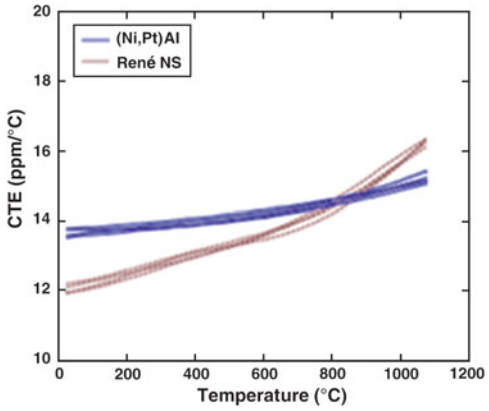


Figure 4. Coefficients of thermal expansion (CTEs) for a commercial diffusion aluminide (Ni,Pt)Al bond coat and its generation 3 René N5 Ni-based superalloy.

with the same phase constituents (γ′ and γ phases) with more optimal compositions for oxidation have been investigated.[46–48] Beyond CTE matching, these systems are desirable due to the lowered driving forces for interdiffusion. However, a drawback is the lower amount of Al available in the coating "reservoir" for TGO formation.

The mechanical properties of bond coatings have a significant influence on their durability in service. Diffusion aluminide coatings have been shown to have a ductile-brittle transition temperature (DBTT) of approximately 600°C. Below the DBTT, the bond coat is linearly elastic with a Young's modulus that depends on composition and is comparable with what has been reported for the β-NiAl phase. Above the DBTT, the ultimate tensile strength and creep response of the diffusion aluminide bond coat is extremely temperature dependent (**Figure 5**a). Strengths of 400 MPa have been measured at intermediate temperatures, but above 1000°C, the strength of commercial diffusion aluminide bond coats does not exceed 50 MPa. Attempts to improve the elevated temperature strength have been only minimally successful, with the greatest high temperature strength being associated with the development of ruthenium aluminide bond coats[49–51] (Figure 5a).

Overlay properties can vary much more widely than those of the diffusion coatings since the composition and microstructure can be more widely varied. Their properties have been somewhat better characterized, since it is possible to deposit very thick layers of the coating (albeit with some loss of similitude of microstructure) and machine conventionally sized test specimens. In general, the physical properties of overlay coatings are similar to those of conventional superalloys. The thermal expansion, particularly of coatings containing Co, tends to be greater than that of superalloys, which tends to increase thermal stresses in these coatings. MCrAlY coatings have been reported to be very strong at room temperature, but their elevated temperature strength is dramatically reduced. Micro-tensile tests of a commercial NiCoCrAlY coating demonstrate impressive room temperature properties with an ultimate tensile strength of 1.4 GPa and significant (>2%) ductility.[52] The strength of these coatings is, however, very temperature dependent and significantly lower than has been measured for diffusion aluminide coatings (Figure 5b).

During service, incorporation of Al into the TGO and continued interdiffusion between the coating and underlying substrate significantly reduces the Al content of the bond coating, which can result in the formation of metastable $L1_0$ martensite phase γ′-Ni_3Al, and eventually γ-Ni. The formation of the $L1_0$ martensite can have a dramatic effect on rumpling if the martensitic (diffusionless) transformation, and attendant volume change, occurs at intermediate temperatures, where the bond coat is easily plastically deformed. The martensite start temperature (M_s) is extremely sensitive to composition and the presence of Pt, which is a common addition to many commercial diffusion aluminide coatings.[53] Without Pt, the martensitic transformation occurs at temperatures well below the β–NiAl DBTT and is stored and recovered elastically. The addition of Pt raises the transformation temperature, which promotes plastic deformation of the bond coat.[54,55]

The TGO is also a key mechanical element of the multilayered system. The TGO undergoes thickening and elongation during the lifetime of the system. The thickening increases the strain energy density, while the elongation provides a driving force for coating failure via the rumpling mechanism.[54,55] TGO elongation results from new TGO forming on internal grain boundaries,[55–57] while thickening is caused by new TGO forming at the TGO/bond-coat interface. The elongation strain

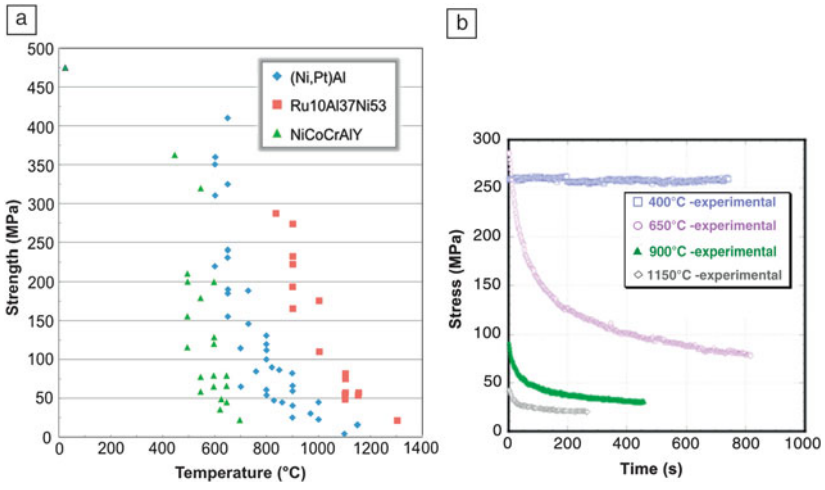


Figure 5. (a) The tensile strength of a NiCoCrAlY overlay bond coat, a platinum modified diffusion aluminide bond coat, and a developmental ruthenium aluminide alloy measured and plotted as a function of temperature. (b) Measured stress relaxations for a diffusion aluminide bond coat. The rate of relaxation above 600°C is impressive, but the relaxation data have been shown to follow conventional models for thermally activated power law creep.

https://doi.org/10.1557/mrs.2012.238 Published online by Cambridge University Press

causes the TGO to develop in-plane compression as it grows. At elevated temperatures, the magnitude of this growth stress is limited by the yield/creep strength of the coating.[9] The growth stresses also provide a key driving force for the sustained peak low cycle fatigue failure mechanism.[56,57] In this scenario, cracks form on the surface of the bond coating, and their faces subsequently oxidize during cycling. These cracks then propagate deep into the substrate by the same oxide elongation processes. The development of the growth stresses in the oxide and the dependence of these stresses on the chemistry of the bond coating are not well understood.

The interface between the TGO and the bond coating is important to the durability of the overall multilayered system. The interface between the TGO and the bond coat is susceptible to decohesion, and this is exacerbated by the segregation of deleterious impurity elements. The most deleterious segregant is S, which at less than 1/3 monolayer coverage causes the work-of-adhesion to be diminished by a factor 10.[58] Conversely, other elements, such as Pt, appear to increase the adhesion,[59,60] though the mechanism is still not well understood. Reactive elements such as Y and Hf also improve adhesion,[60,61] but again their distribution within the coating and at the interface and the mechanism(s) by which they improve adhesion require further fundamental study. In general, the chemical environment at the interfaces and its influence on interfacial toughness is still not well understood.

New design and characterization tools

Optimization of the composition and properties of each coating layer remains a major challenge. Calphad thermodynamic phase equilibria tools that provide insights to the thermodynamically stable phases that exist at elevated temperature as a function of composition (Figure 1) can be used to guide the design of new systems. However, since the superalloy substrate may contain 8–10 elements and the coating often contains an additional 3–6 elements, the thermodynamic assessments of all the potential phases are often not accurate enough to predict the structure of the coating. With regard to kinetics and the prediction of structure evolution, limited interdiffusion data in the relevant range of composition represents a major constraint. First principles computational techniques can now be employed to investigate atomic hop mechanisms in multicomponent systems. Combined with cluster expansions and Monte Carlo simulations, it is possible to predict macroscopic diffusion coefficients, including the large variations in diffusivity with departures from stoichiometry in NiAl.[62–65] Such approaches hold promise for the design of coatings that resist interdiffusion.

When incomplete information on phase equilibria and interdiffusion behavior exists, combinatorial experimental approaches are useful. **Figure 6**a shows 45 coating samples placed in an ion plasma deposition system among three cathodes, each of a different composition. The resultant distribution of Pd with a Cathode 1 composition of Ni-46Al-4Cr-12Pd (and other cathodes Pd-free) is shown in Figure 6b. In this manner, the influence of Pd in a B2 type coating can be explored over a wide range of composition within a single coating deposition cycle.

The mechanical properties of the coating layers have proven to be extremely difficult to measure experimentally, owing to their reduced dimensionality, propensity to interact and evolve with thermal cycling, and the need to measure these properties at both room and elevated temperatures. MEMS (microelectromechanical systems)-inspired techniques have led to the implementation of micro-tensile testing as a reliable means for elucidating the constitutive behavior of individual TBC layers. Freestanding bond coats can be prepared by chemically etching away the ceramic topcoat and TGO, scalping 500-μm slices of bond coat with a thin layer of superalloy from the underlying substrate with electro-discharge machining, and then lapping and polishing to remove the underlying superalloy.[45] Bow tie shaped micro-tensile specimens can be cut and individually ground and polished to a thickness of 20–50 μm with all unwanted layers (topcoat, TGO, and substrate) removed, **Figure 7**a. For measurement of mechanical properties, custom micro-tensile piezoelectric driven load frames have been developed, Figure 7a. Thermal and electrical isolation of the grips from the load frame allow for resistive heating. Young's modulus, yield, and ultimate tensile strengths and strain to failure have been measured from full micro-tensile stress-strain curves. Time-dependent creep properties can also be measured by loading in tension, fixing the grips, and recording the changes in stress and strain that occur as a function of time for characterization of power law creep constitutive relationships.[45]

Location specific measurements of room temperature mechanical response can also be measured using nanoindentation and micropillar compression testing, Figure 7b–c. These pillars may be machined within individual layers normal to the growth direction using focused ion beam systems[66] or by recently developed femtosecond laser micromachining

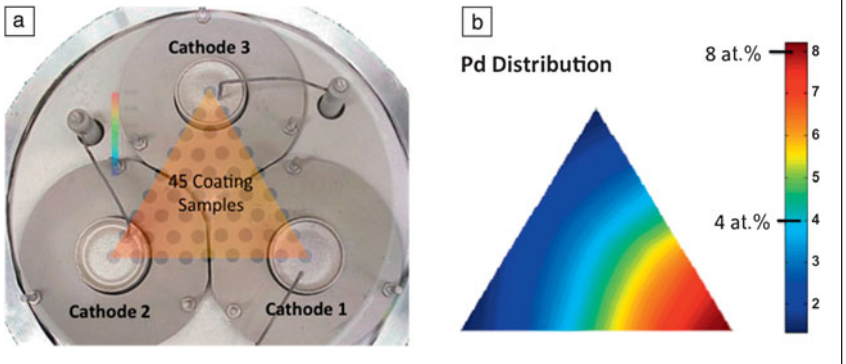


Figure 6. (a) Combinatorial matrix of 45 samples fabricated from three cathodes of different compositions in an ion plasma deposition system, and (b) the distribution of Pd across the set of 45 samples with Cathode 1 containing 12 at.% Pd and Cathodes 2 and 3 containing no Pd.

https://doi.org/10.1557/mrs.2012.238 Published online by Cambridge University Press

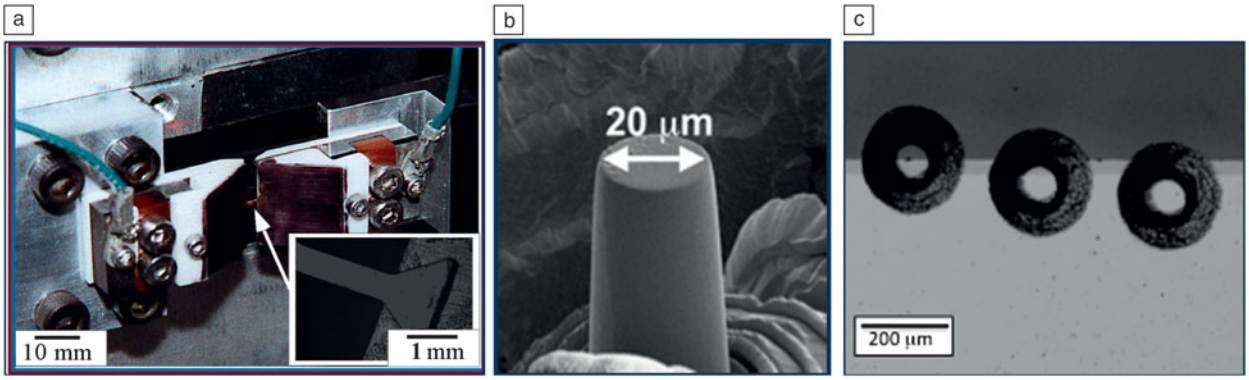


Figure 7. (a) Freestanding diffusion aluminide bond coat micro-tensile specimen mounted in a custom build load frame, resistively heated and ready for tensile testing, (b) micropillar machined with femtosecond laser, and (c) a series of micropillars machined across a coating interface.

methods.[67,68] A well-developed methodology of compressing these pillars with flat diamond microindentors[66] permits acquisition of room temperature properties of the coatings. With size-scale effects properly accounted for, these techniques provide location specific measures of modulus, hardness, and strength, but they are currently limited to room temperature measurement. Other location-specific measurements for properties such as thermal conductivity have also recently been developed.[69,70] Prospects for intermediate temperature testing are promising, but these techniques are far from being used at temperatures of 1000°C.

As mentioned previously, the TGO, typically alumina, is a key element of the multilayered system that must adhere to the bond coating to provide an environmental barrier and to maintain adherence of the ceramic topcoat. Optical spectroscopy tools offer non-contact, non-destructive evaluation of the state of the TGO during cycling.[71–75] Luminescence lines generated by laser illumination undergo a stress-induced frequency shift due to the presence of very small quantities of naturally occurring Cr^{3+} as an impurity. Analysis of the luminescence spectrum permits assessment of the stresses in the TGO, which are compressive and of the order of 100–400 MPa at elevated temperature and rise beyond 4 GPa at room temperature due to the CTE mismatch with the superalloy substrate.[57,77,78] With recently incorporated scanning capabilities, new piezospectroscopy tools can analyze the spatial variations in stress as well as assess subsurface damage that alters the stress state in the oxide.[73–76] An example of the spatial variation in stresses is shown for a platinum aluminide coating oxidized at 1093°C, **Figure 8**, where the compressive stresses in the oxide range from 3–7 GPa following cooling to room temperature. Synchrotron x-ray experiments have additionally been employed to observe the development and evolution of growth stresses *in situ* at elevated temperatures.[77,78]

Future challenges and opportunities

Building the infrastructure to design multicomponent bond coatings that perform in a predictable manner within the multilayered thermal-barrier coating (TBC) system remains a major challenge. The bond-coat element of the TBC system has traditionally been developed in isolation from the substrate and the ceramic topcoat with limited measurement of properties as a function of composition. This can lead to substantial debits in performance when combined with system elements. Emerging

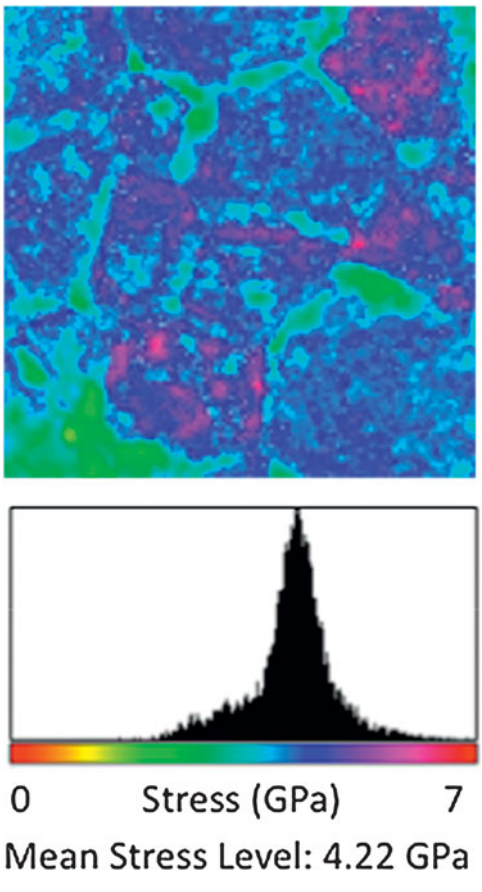


Figure 8. Stresses in a PtAl coating after oxidation at 1093°C /160 h and subsequent cooling to room temperature measured by confocal piezospectroscopy.

https://doi.org/10.1557/mrs.2012.238 Published online by Cambridge University Press

tools with improved capabilities for predicting and measuring properties, some described in the previous sections and some yet to be developed, will contribute positively to this challenge. The properties of interfaces within the system remain as a barrier to predicting system performance.

The drive toward higher-efficiency (i.e., hotter-running, more highly stressed) engines, unconventional propulsion fuels, and reduced reliance on exotic materials will motivate these new tools for optimizing system performance as well as new coatings with the following characteristics:

- Multi-component coatings for turbine parts with internal passages that are not amenable to line-of-sight overlay coating processes
- Multi-functional coatings capable of location-specific response
- Coatings that possess load-bearing capability, which are increasingly important as aero components move to thinner walls
- Coating processes that are amenable to field application (e.g., high-agility thermal spray processes that can be employed for localized repair)
- Reduced cost coatings that contain limited amounts of Pt and other costly/scarce materials that can be applied with low-capital processing equipment, flexible chemistry, and simplification of manufacturing processes (fewer process steps, scalable equipment, low maintenance).

Finally, with regard to system performance, experience with existing bond-coat/TBC systems has illustrated a competition between failure mechanisms that depend strongly on the plastic properties of the bond coat, the interface fracture toughness governing bond coat/TGO or TGO/TBC failure, and the fracture toughness of the ceramic topcoat.[2,8,9] In order to speed system development and deployment, simulations are needed to help anticipate such competitions and identify material combinations that balance multiple failure mechanisms. Conventional approaches to simulate interface and coating failure processes are not well suited to this task because they require explicit *a priori* definition of the failure mode, including multiple crack geometries, computation of the associated energy release rates, and the post-*priori* assessment of stability (by comparing driving forces to toughness). Coupled with the need to conduct simulations for a broad material parameter space, there is a critical need for an efficient alternative approach that reduces the number of simulations required to identify active failure mechanisms in terms of system properties. Parallel computing approaches are likely to advance these systems-based challenges.

Acknowledgments

T.P. is grateful for the support of an NSF-GOALI program DMR-11–05672.

References

1. R.C. Reed, *The Superalloys: Fundamentals and Applications* (Cambridge University Press, UK, 2006).
2. A.G. Evans, D.R. Clarke, C.G. Levi, *J. Eur. Ceram. Soc.* **28** (7), 1405 (2008).
3. S.M. Meier, D.K. Gupta, *Trans. ASME* **116**, 250 (1994).
4. U. Schulz, C. Leyens, K. Fritscher, M. Peters, B. Saruhan-Brings, O. Lavigne, M. Dorvaux, M. Poulain, R. Mévrel, M.L. Caliez, *Aerosp. Sci. Technol.* **7** (1), 73 (2003).
5. T. DeMasi-Marcin, D.K. Gupta, *Surf. Coat. Technol.* **68/69**, 1 (1994).
6. J.R. Nicholls, *MRS Bulletin* **28**, 659, (2003).
7. M.J. Stiger, N.M. Yanar, M. Topping, F.S. Pettit, G.H. Meier, *Z. Metallkd.* **90**, 1069 (1999).
8. P.K. Wright, A.G. Evans, *Curr. Opin. Solid State Mater. Sci.* **4**, 255 (1999).
9. A.G. Evans, D.R. Mumm, J.W. Hutchinson, G.H. Meier, F.S. Pettit, *Prog. Mater Sci.* **46**, 505 (2001).
10. R.T. Wu, K. Kawagishi, H. Harada, R.C. Reed, *Acta Mater.* **14**, 3622 (2008).
11. J.G. Smeggil, A.W. Funkenbush, N.S. Bornstein, *Metall. Trans. A* **17**, 923 (1986).
12. J.L. Smialek, in *Microscopy of Oxidation 3*, S.B. Newcomb, J.A. Little, Eds. (The Institute of Materials, London, UK, 1996), p. 127.
13. P.Y. Hou, *Oxid. Met.* **52**, 337 (1999).
14. I.G. Wright, B.A. Pint, W.Y. Lee, K.B. Alexander, K. Prüssner, in *High Temperature Surface Engineering* (The Institute of Materials, London, UK, 2000), p. 95.
15. G.W. Goward, L.W. Cannon, ASME Paper 87-GT-50 (ASME, New York, 1988).
16. G.M.C.A. Gauje, US Patent 3,486,927 (1969).
17. D.J. Levine, M.A. Levinstein, US Patent 3,540,878 (1970).
18. D.J. Levine, US Patent No. 3,598,638 (1971).
19. R.L. Wachtell, C.A. De Guisto, US Patent No. 3,073,015 (1963).
20. R. Bianco, R.A. Rapp, *J. Electrochem. Soc.* **140** (4), 1181 (1993).
21. R.G. Wing, I.R. McGill, *Platinum Met. Rev.* **25** (3), 94 (1981).
22. J.S. Smith, D.H. Boone, ASME Paper 90-GT-319 (ASME, 1990).
23. P.C. Patnaik, R. Thamburaj, T.S. Sudarshan, in *Surface Modification Technologies III*, T.S. Sudarshan, D.G. Bhat, Eds. (TMS, Warrendale, PA, 1990), p. 759.
24. T.E. Strangman, US Patent 5,514,482 (1996).
25. I.R. McGill, G.L. Selman, US Patent 4,399,199 (1983).
26. G.J. Tatlock, T.J. Hurd, *Oxid. Met.* **22**, 201 (1984).
27. B.A. Nagaraj, W.B. Connor, R.W. Jendrix, D.J. Wortman, L.W. Plemmons, US Patent 5,427,866 (1995).
28. D.S. Rickerby, S.R. Bell, R.G. Wing, US Patent 5,667,663 (1997).
29. S. Sampath, X.Y. Jiang, J. Matejicek, L. Prchlik, A. Kulkarni, A. Vaidya, *Mater. Sci. Eng., A* **364**, 216 (2004).
30. D.H. Boone, S. Shen, R. McKoon, *Thin Solid Films* **64** (2), 299 (1979).
31. S. Shankar, D.E. Koenig, L.E. Dardi, *J. Met.* **33** (10), 13 (1981).
32. J.E. Jackson, US Patent No. 3,470,347 (1969).
33. T.A. Taylor, M.P. Overs, B.J. Gill, R.C. Tucker, *J. Vac. Sci. Technol., A* **3** (6), 2526 (1985).
34. J.A. Browning, US Patent 5,120,582 (1992).
35. L. Russo, M. Dorfman, in *Proceedings of the International Thermal Spray Conference*, A. Ohmori, Ed. (High-Temperature Society of Japan, 2002), p. 1179.
36. V. Baranovski, A. Verstak, US Patent 6,245,390 (2001).
37. T. Stoltenhoff, H. Kreye, H.J. Richter, *J. Therm. Spray Technol.* **11** (4), 542 (2002).
38. Y. Ichikawa, K. Sakaguchi, K. Ogawa, T. Shoji, S. Barradas, M. Jeandin, M. Boustie, in *Thermal Spray 2007: Global Coating Solutions*, B.R. Marple, M.M. Hyland, Y.-C. Lau, C.-J. Li, R.S. Lima, G. Montavon, Eds. (ASM International, Materials Park, OH, 2007), p. 54.
39. M.F. Smith, A.C. Hall, J.D. Fleetwood, P. Meyer, *Coatings* **1**, 117 (2011).
40. E.N. Kablov, S.A. Muboyadzhyan, S.A. Budinovskii, A.N. Lutsenko, *Russ. Metall.* **5**, 364 (2007).
41. J. Vetter, O. Knotek, J. Brand, W. Beele, *Surf. Coat. Technol.* **68–69**, 27 (1994); O. Knotek, E. Lugscheider, F. Löffler, W. Beele, C. Barimani, *Surf. Coat. Technol.* **74–75**, 118(1995).
42. J.-C. Zhao, D.M. Lipkin, US Patent 6,964,791 (2005).
43. D.S. Balint, J.W. Hutchinson, *Acta Mater.* **51**, 3965 (2003).
44. D.S. Balint, J.W. Hutchinson, *J. Mech. Phys. Solids* **53**, 949 (2005).
45. D. Pan, M.W. Chen, P.K. Wright, K.J. Hemker, *Acta Mater.* **51**, 2205 (2003).
46. I. Takeshi, B. Gleeson, *J. Jpn. Inst. Met.* **71**, 34 (2007).
47. A. Sato, H. Harada, K. Kawagishi, *Metall. Mater. Trans. A* **37**, 790 (2006).
48. K. Kawagishi, H. Harada, A. Sato, K. Matsumoto, *Superalloys* 76 (2008).
49. B. Tryon, F. Cao, K.S. Murphy, C.G. Levi, T.M. Pollock, *JOM* **58**, 53 (2006).
50. B. Tryon, Q. Feng, R. Wellman, K. Murphy, J. Yang, C. Levi, J. Nicholls, T.M. Pollock, *Metall. Mater. Trans. A* **37**, 3347 (2006).
51. F. Cao, T.M. Pollock, *Metall. Mater. Trans. A* **39**, 39 (2008).
52. K.J. Hemker, B.G. Mendis, C. Eberl, *Mater. Sci. Eng., A* **483–484**, 727 (2008).
53. M.W. Chen, M.L. Glynn, R.T. Ott, T.C. Hufnagel, K.J. Hemker, *Acta Mater.* **51**, 4279 (2003).
54. A.M. Karlsson, J.W. Hutchinson, A.G. Evans, *Mater. Sci. Eng., A* **351**, 24 (2003).
55. D.R. Mumm, A.G. Evans, I.T. Spitsberg, *Acta Mater.* **49**, 2329 (2001).

https://doi.org/10.1557/mrs.2012.238 Published online by Cambridge University Press

56. A. Suzuki, M.F.X. Gigliotti, B.T. Hazel, D.G. Konitzer, T.M. Pollock, *Metall. Mater. Trans. A* **41**, 948 (2010).
57. A.G. Evans, M.Y. He, A. Suzuki, M. Gigliotti, B. Hazel, T.M. Pollock, *Acta Mater.* **57**, 2969 (2009).
58. W. Zhang, J.R. Smith, X.-G. Wang, A.G. Evans, *Phys. Rev. B* **67** (245414), 1 (2003).
59. B.A. Pint, I.G. Wright, W.Y. Lee, Y. Zhang, K. Prüßner, K.B. Alexander, *Mater. Sci. Eng., A* **245**, 201 (1998).
60. B. Pint, J.A. Haynes, T.M. Besmann, *Surf. Coat. Technol.* **204**, 3287 (2010).
61. J.L. Smialek, in *Proc. Electrochemical Society: Symposium on High Temperature Corrosion and Materials Chemistry*, P.Y. Hou, M.J. McNallan, R. Oltra, E.J. Opila, D.A. Shores, Eds. (Electrochemical Society, Pennington, NJ, 1998), pp. 211–220.
62. Q. Xu, A. Van der Ven, *Acta Mater.* **59**, 1095 (2011).
63. A. Van der Ven, J.C. Thomas, Q. Xu, J. Bhattacharya, *Math. Comput. Simul.* **80** (7), 1393 (2010).
64. Q. Xu, A. Van der Ven, *Phys. Rev. B* **81**, 064303 (2010).
65. Q. Xu, A. Van der Ven, Intermetallics **17** (5), 319 (2009).
66. M.D. Uchic, D.M. Dimiduk, J.N. Florando, W.D. Nix, *Science* **305**, 986 (2004).
67. Q. Feng, Y.N. Picard, H. Liu, S.M. Yalisove, G. Mourou, T.M. Pollock, *Scripta Mater.* **53**, 511 (2005).
68. S. Ma, B. Tryon, J.P. McDonald, S.M. Yalisove, T.M. Pollock, *Metall. Mater. Trans. A* **38**, 2153 (2007).
69. X. Zheng, D.G. Cahill, R. Weaver, J.-C. Zhao, *J. Appl. Phys.* **104**, 073509 (2008).
70. J.-C. Zhao, *Prog. Mater Sci.* **51**, 557 (2006).
71. S.H. Margueron, D.R. Clarke, *Acta Mater.* **54**, 5551 (2006).
72. D.R. Clarke, D.J. Gardiner, *Int. J. Mater. Res.* **98**, 8 (2007).
73. V.K. Tolpygo, D.R. Clarke, K.S. Murphy, *Surf. Coat. Technol.* **188–189**, 62 (2004).
74. D.R. Clarke, *Curr. Opin. Solid State Mater. Sci.* **6**, 237 (2002).
75. V. Sergo, D.R. Clarke, *J. Am. Ceram. Soc.* **81**, 3237 (1998).
76. V.K. Tolpygo, J.R. Dryden, D.R. Clarke, *Acta Mater.* **46**, 927 (1998).
77. P.Y. Hou, A.P. Paullikas, B.W. Veal, *Mater. Sci. Forum* **522–523**, 433 (2006).
78. D. Hovis, L. Hu, A. Reddy, A.H. Heuer, A.P. Paullikas, B.W. Veal, *Int. J. Mater. Res.* **98**, 12 (2007). □

The Materials Research Society
is proud to announce the

MATERIALS RESEARCH SOCIETY
FOUNDATION

Unique in several ways, the Foundation:

- advances the MRS mission to "promote communication for the advancement of interdisciplinary materials research to improve the quality of life"
- focuses on member engagement and funding to enrich, expand and ensure MRS core programs in education, outreach and peer recognition
- leverages corporate partner, institutional and individual support to invest in projects of importance to the materials community, as defined by the materials community
- benefits a wide range of innovative grassroots, member-driven initiatives—from student chapter proposals, to local or regional education/outreach projects, to those with the potential to impact the materials enterprise worldwide.

To learn how you can help make a difference or to apply for project funding, explore the Foundation website, **www.mrs.org/foundation.** The first project grants will be awarded at the 2013 MRS Spring Meeting in San Francisco.

The Materials Research Society Foundation operates as a program of the Materials Research Society. The official registration and financial information of the Materials Research Society Foundation may be obtained from the Pennsylvania Department of State by calling toll free, within Pennsylvania, 1.800.732.0999. Registration does not imply endorsement.

https://doi.org/10.1557/mrs.2012.238 Published online by Cambridge University Press